ISSN 0001-4338, Izvestiya, Atmospheric and Oceanic Physics, 2013, Vol. 49, No. 4, pp. 439–449. © Pleiades Publishing, Ltd., 2013.
Original Russian Text © A.M. Chukharev, 2013, published in Izvestiya AN. Fizika Atmosfery i Okeana, 2013, Vol. 49, No. 4, pp. 477–488.

Multitime Scale Model of Turbulence in the Sea Surface Layer

A. M. Chukharev

Marine Hydrophysical Institute, National Academy of Sciences of Ukraine, ul. Kapitanskaya 2, Sevastopol, 99011 Ukraine
e-mail: alexchukh@ukr.net

Received May 14, 2012; in final form, August 24, 2012

Abstract—A model has been developed to describe the turbulent structure of the surface layer which takes into account the differences in the scales of turbulent vortices generated by different mechanisms. We consider the shear of the drift current, nonlinear effects of surface waves, and their breaking as the main sources of turbulent energy. The power spectrum is divided into ranges with respect to the scales. The equation system for each range is solved numerically. The modeling results are compared with the experimental data and with other currently known models. The advantages of the suggested approach are demonstrated.

Keywords: turbulence, air-sea interaction, multiscale model, energy dissipation, surface layer, generation mechanisms

DOI: 10.1134/S0001433813040026

INTRODUCTION

Describing the turbulent structure in neighboring layers of two media is a very complicated problem owing to the strong variability and variety of processes occurring near the boundary between the sea and the atmosphere. In the last decades, significant progress was made in the experimental and theoretical research of marine turbulence near the surface. New important results were obtained that give a more complete concept about the physical processes occurring in this layer.

Special experiments on the investigation of turbulence in the layer of wind waves were described in [1–3]. They used the linear filtration of the turbulent and wave velocity components. According to the data of these investigations, the peak on the spectrum of turbulent pulsations is located near the dominating wave frequency. The estimates demonstrated that neither filtration errors nor effects of nonlinearity of the surface waves can make such a contribution. It is most likely that this effect is related to the energy transfer from the waves to turbulence by means of interaction. However, it does not explain the existence of the peak at this frequency, because turbulence generated by the shear has notably lower frequencies. An estimate of the dissipation rate of turbulent energy in [2] showed that $\varepsilon \sim 1$ cm^2/s^3 is two orders of magnitude greater than the value expected for the layer of constant stress:

$$\varepsilon = \frac{u_*^3}{\kappa z} \approx 10^{-2} \text{ cm}^2/\text{s}^3, \quad (1)$$

where u_* is the dynamic velocity in water, $\kappa = 0.4$ is the von Karman constant, and z is depth. The enhanced values of the dissipation rate can be explained only by other sources (besides shear): breaking waves and the interaction between waves and turbulence.

The results of experimental and theoretical studies [3–5] formed a concept about the multilayer structure of turbulence under the surface of the sea. At present, a three-layer scheme of dissipation distribution is considered the most realistic one: in the upper layer, the dissipation rate is approximately constant; it is determined by the influence of breaking waves. An intermediate layer or transition layer is located below it, where $\varepsilon \sim z^{-2}$; below that, the depth dependence of ε becomes similar to the layer near a wall: $\varepsilon \sim z^{-1}$ [3]. The depth of the upper zone is $z_b \approx 0.6H_s$ (H_s is the height of significant waves). Approximately half of the entire energy dissipation occurs here. The depth of the transition layer is $8.3 < z_t/H_s < 13$. A theoretical description of such a three-layer scheme based on the similarity laws is given in [6].

It was found in the investigations reported in [7] that experimentally measured energy dissipation under the sea surface is sometimes in a good agreement with relation (1), but frequently the values of ε are notably higher. The authors suggested two mechanisms to explain this phenomenon: (1) the turbulence is generated by wave breaking and then transported deeper by the wave motions and swell, and (2) the energy of the vortex waves is transmitted to the mean current and later transfers to turbulence. The influence of waves on the turbulence was considered in [8], where it was shown that a significant part of energy lost by waves goes to generating turbulence through the shears caused by the Stokes drift.

Many investigators have reported about the special role of breaking waves in the turbulization of the upper

layer of the ocean [1, 9]. This mechanism sharply increases turbulence generation and intensifies the exchange processes between the sea and atmosphere. A model was suggested in [10] to estimate the influence of breaking waves on the resistance of the water surface and redistribution of energy over the spectrum.

A model developed by Craig and Banner [4, 5] was an important step in the generation of the theoretical concepts. In order to close the equation system in the model, the authors used a Prandtl hypothesis about the pathway of mixing (turbulence scale). The calculations using this model demonstrated the agreement both with the field data [1] and laboratory experiments. The results depended strongly on the value of the roughness parameter (z_0) and on the selection of the turbulence scale (l). The layer near the surface with increased dissipation rate was interpreted as a consequence of the turbulent-energy flux from the waves through the surface. The field data obtained in [11] were also described well by the model, but the values of z_0 were much smaller.

The closure of the equation system for the turbulent kinetic energy balance and dissipation rate of the turbulent energy by means of expressing the viscosity coefficient as functions of energy and dissipation was used in [12] and in [13], where the Launder model (k–ε model) was used as the basis. In both cases the shear of currents and surface waves were considered turbulence sources. However, the terms describing the wave energy transformation and the interaction of waves with turbulence were parameterized differently. The disadvantage of this model is the absence of an explicit account for wave breaking, which leads to limitations of their application.

On the contrary, the authors of [14] consider that wave breaking, including microbreaking, is the main source of turbulent energy in the utmost upper layer of the sea. This phenomenon is considered the volume source of energy and momentum, depending on the spectral composition of surface waves. It is assumed that diffusion is neglected in the turbulent-energy balance.

Many questions remain unsolved despite much attention focused on the problems of marine turbulence and progress made over the last few years in the investigation of the surface sea layer and its interaction with the atmosphere. We cannot consider that our concepts about the structure of turbulence, the role of individual generation mechanisms, and the variation in the turbulence intensity in different hydrometeorological conditions are final. The existence of waves that differ by in spectral composition; influence of the swell; different directions of wind, currents, and waves; and the role of stratification and heat fluxes make up an incomplete list of the problems that require additional investigation. The development of adequate models for the surface layer will allow a more exact forecast of the response of the sea to atmospheric forcing and allow us to estimate the fluxes of heat, momentum, and other substances in this layer. The investigations on small scales are needed for the correct parameterization of the physical processes that occur near the interface between the two media and including these data as the sub-grid values in large-scale models of the interaction between the ocean and the atmosphere and also in the regional climatic models.

The objective of this work is to develop a model for calculating the depth distribution of turbulent energy and dissipation rate in the surface layer of the sea using concepts of the multiscale processes of turbulence generation by different mechanisms and the cascade transport of energy into the dissipation range. We suggest dividing the energetic spectrum of turbulence into ranges in which we can write an individual system of equations and obtain numerical solutions.

A PHYSICAL MODEL

The approach based on the hypotheses of Kolmogorov about the turbulent-energy dissipation rate is currently most frequently used to describe turbulence. The time scale corresponding to the interactions between velocity pulsations can be determined from the turbulent kinetic energy and dissipation rate as $T \sim E_t/\varepsilon$. It is assumed in the equilibrium models that the entire energy transported to the turbulence in the large-scale range is transported at the same rate over the spectrum to smaller scales and finally dissipates. Although it is generally accepted that a spectrum of turbulent pulsations scales exist, most single-point models consider only one time scale.

An approach to the calculation of turbulent currents was suggested in [15] using many time scales which characterize the rates of development of different turbulent interactions. The energy containing a spectrum range is divided into ranges with different responses to variations in the surrounding medium and different dissipation rates. The authors considered the division of the spectrum into three ranges: generation of energy, transfer, and dissipation. The results of modeling demonstrated an "amazing improvement" of the coincidence between calculations and experiments.

Several mechanisms of turbulence generation exist in the surface layer of the sea that operate in different spectral ranges. Therefore, it is reasonable to consider the influence of each of them precisely in the corresponding range. In some sense, a similar idea of division the spectrum into ranges in which the energy is generated and that are divided by inertial ranges where the "–5/3" law is valid was developed by Ozmidov [16]. In this work, we shall limit ourselves by the consideration od three mechanisms of generation, which are considered most important from the energetic point of view [9] in the surface layer: instability of the vertical gradients of the drift current (shear), hydrodynamic instability of the surface waves, and wave break-

ing. The turbulent vortices generated by velocity shear are comparatively "slow," but their spatial scales are sufficiently large and can reach tens of meters [9]. The turbulence caused by wave breaking and nonlinear wave effects is "faster"; its special scales are smaller but the intensity of wave energy transformation to turbulence, especially due to wave breaking, can be significant. It is likely that there are no sufficient grounds to divide the latter two mechanisms by their scales; therefore, we shall limit ourselves by the assumption that they are close. The influence of the surface waves on the turbulent regime (without the analysis of breaking) was discussed in detail in [17], where it was noted that the main effect of the wave interaction with turbulence is the vertical transport of kinetic energy by turbulent pulsations. It is likely that the main role is played by the motions whose scale is comparable with the thickness of the wave layer. An estimate of the time scales related to the shear turbulence T^{sh} and to the wave motions T^{w} shows that $T^{sh} \gg T^{w}$ [17].

Figure 1 shows a scheme of the characteristic power spectrum of turbulence near the sea surface and suggested division it into the parts, in which turbulence is generated by different mechanisms, its inertial transport to the range of higher wave numbers, and dissipation. Let us consider that the production of turbulent energy occurs in ranges 1 and 2, which are characterized by the corresponding energy levels E_{P1} and E_{P2}. Part of the energy from these ranges is transformed with rates ε_{P1} and ε_{P2} to the energy of smaller scale pulsations supplementing the energy in ranges 2 and 3, respectively. Energy transport with rates ε_{T3} occurs in wave number range $k_2 \le k \le k_3$. The energy level in this range is denoted as E_{T3}. This range is considered inertial; there is no turbulent-energy generation. The fourth spectral range is dissipative. It is located in the wave numbers range $k \ge k_3$. In the first range of scales, turbulence is generated by the shear of the drift current; in the second range, generation occurs due to the nonlinear effects of surface waves and their breaking. In the scheme, these energy inflows are denoted as P_1 and P_2, respectively. We assume that the total turbulent energy is distributed between ranges 1–3, and a negligible part corresponds to the fourth range. In order to highlight the peculiarities of the ranges considered here, letters are added to the indices at ε and E, which indicate that the production of energy occurs here (index P) or is transferred (index T).

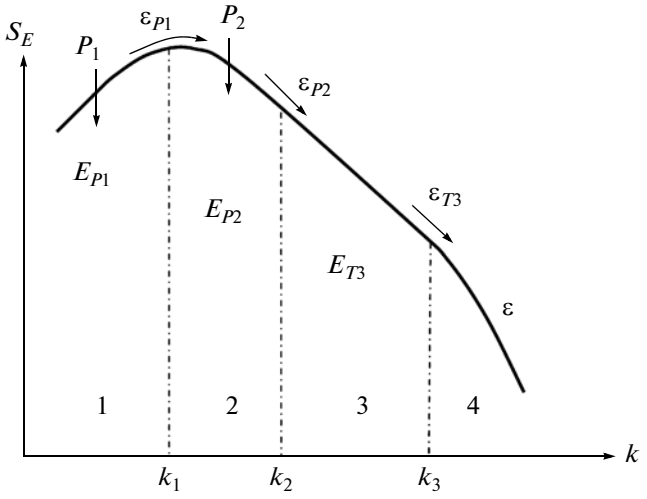

Fig. 1. Scheme of dividing the spectrum into ranges.

DERIVATION OF THE MODEL EQUATIONS

Let us use the equations of the turbulent kinetic energy conservation and dissipation rate to describe the turbulence in each of the ranges; i.e., we shall use the well known k–ε model [18]. Taking into account our assumptions, we shall write the initial equations for these values in the first range as

$$\frac{\partial E_{P1}}{\partial t} + U_i \frac{\partial E_{P1}}{\partial x_i} = -\overline{u_i' u_j'} \frac{\partial U_i}{\partial x_j} + C_E \frac{\partial}{\partial x_k}\left(\overline{u_k' u_l'} \frac{E_{P1}}{\varepsilon_{P1}} \frac{\partial E_{P1}}{\partial x_l}\right) - \varepsilon_{P1}; \quad (2)$$

$$\frac{\partial \varepsilon_{P1}}{\partial t} + U_i \frac{\partial \varepsilon_{P1}}{\partial x_i} = C_1 \frac{\varepsilon_{P1}}{E_{P1}}\left(\overline{u_i' u_j'} \frac{\partial U_i}{\partial x_j}\right) + C_\varepsilon \frac{\partial}{\partial x_k}\left(\overline{u_k' u_l'} \frac{E_{P1}}{\varepsilon_{P1}} \frac{\partial \varepsilon_{P1}}{\partial x_l}\right) - C_2 \frac{\varepsilon_{P1}^2}{E_{P1}}. \quad (3)$$

Here, $\overline{u_i' u_j'}$ are kinematic Reynolds stresses, C_i are constants, and U_i are components of the main velocity. We neglect the Coriolis force, molecular viscosity, and pulsations of pressure. In the stationary case, we consider the current horizontally uniform and apply the hypothesis of gradient diffusion. Equations (2) and (3) are simplified and reduced to the following model form:

$$\nu_1^t \left(\frac{dU}{dz}\right)^2 + \frac{d}{dz}\left(\frac{\nu_1^t}{\sigma_E} \frac{dE_{P1}}{dz}\right) - \varepsilon_{P1} = 0, \quad (4)$$

$$C_1 \frac{\varepsilon_{P1}}{E_{P1}} \nu_1^t \left(\frac{dU}{dz}\right)^2 + \frac{d}{dz}\left(\frac{\nu_1^t}{\sigma_\varepsilon} \frac{d\varepsilon_{P1}}{dz}\right) - C_2 \frac{\varepsilon_{P1}^2}{E_{P1}} = 0, \quad (5)$$

where the Reynolds stresses are expressed as functions of the turbulent viscosity coefficient ν^t and gradient of the mean velocity current: $-\overline{u_i' u_j'} = \nu^t \frac{dU}{dz}$, σ_E, and σ_ε are constants. The physical sense of the terms in Eq. (4) is as follows: the first describes turbulence generation by the velocity shear, the second describes dif-

fusion of the turbulent kinetic energy, and the third describes the rate of energy transfer to the second range of scales. The first term in Eq. (5) describes the production of dissipation, the second describes diffusion, and the third describes the rate of dissipation transfer. The system is closed by the expression of the turbulent viscosity coefficient through the turbulent kinetic energy and dissipation: $\nu^t = C_\mu \frac{E^2}{\varepsilon}$. Constant C_μ is usually assumed equal to 0.09 [18]. We admit that horizontal current $U(z)$ is generated by the tangential wind stress at the surface; i.e., the velocity profile of the drift current is expected to be close to a logarithmic one:

$$U(z) \approx U_0 - \frac{u_*}{\kappa}\ln\left(\frac{z+z_0}{z_0}\right), \tag{6}$$

where κ is the von Karman constant; u_* is friction velocity in water, which was calculated through the friction velocity in the air: $u_* = \sqrt{\rho_a/\rho_w}u_*^a$, $u_*^a = \sqrt{c_D}V_{10}$, ρ_a and ρ_w are densities of air and water; c_D is the resistance coefficient of the surface; and V_{10} is wind velocity at a height of 10 m. The following boundary conditions are accepted:

$$\begin{aligned} &E_{P1} = E_{01}, \quad \varepsilon_{P1} = \varepsilon_{01} \text{ at } z = 0, \\ &\frac{dE_{P1}}{dz} = \frac{d\varepsilon_{P1}}{dz} = 0 \text{ at } z \to \infty. \end{aligned} \tag{7}$$

In the second range of scales, where $k_1 \le k \le k_2$, the model equations with the account for all conditions indicated above would be written as

$$\varepsilon_{P1} + P^w + qP^{br} + \frac{d}{dz}\left(\frac{\nu_1^t}{\sigma_E}\frac{dE_{P2}}{dz}\right) - \varepsilon_{P2} = 0, \tag{8}$$

$$\begin{aligned} &C_3\frac{\varepsilon_{P2}}{E_{P2}}\left(\varepsilon_{P1} + P^w + qP^{br}\right) \\ &+ \frac{d}{dz}\left(\frac{\nu_1^t}{\sigma_\varepsilon}\frac{d\varepsilon_{P2}}{dz}\right) - C_4\frac{\varepsilon_{P2}^2}{E_{P2}} = 0. \end{aligned} \tag{9}$$

We denote the energy input to turbulence due to the nonlinear effects of surface waves and due to their breaking as P^w and P^{br}, respectively; q is the probability of breaking. Thus, the first three terms in Eq. (8) describe the energy input; the sense of the other terms in the equations is similar to Eqs. (4) and (5). From the equation of the wave kinetic energy balance, we get [19]

$$-\frac{\partial F^w}{\partial x_3} - \tau_\alpha^w\frac{\partial U_\alpha}{\partial x_3} + \overline{\tilde\tau_{ij}^t\frac{\partial\tilde u_i}{\partial x_j}} = 0, \tag{10}$$

where $F^w = \frac{\partial}{\partial z}\left(\overline{u_3' E_w}\right) = -\nu^t\frac{\partial E^w}{\partial x_3}$ and $\tau_\alpha^w = \overline{\tilde u_\alpha\tilde u_3}$ are vertical fluxes of energy and momentum of wave motions, respectively; $\overline{\tilde\tau_{ij}^t\frac{\partial\tilde u_i}{\partial x_j}} = P^w$ is the production of turbulent energy by wave motions; $\tilde\tau_{ij}^t$ are wave modulations of the turbulent momentum flux; and $E^w = \frac{\overline{\tilde u_i\tilde u_i}}{2}$ is the wave energy. For the flat case (two-dimensional waves), we find that

$$P^w(z) = \frac{d}{dz}\left(\frac{\nu^t}{\sigma_w}\frac{dE^w}{dz}\right) + \overline{\tilde u_1\tilde u_3}\frac{dU}{dz}. \tag{11}$$

The values of $\tilde u_i$ and E^w are found from the linear wave theory, σ_w is a constant. The second term in the right part of (11) determines the energy transfer from the wave field to the mean current. According to the laboratory studies in [20], stresses $\overline{\tilde u_i\tilde u_3}$ induced by waves are negative. They are smaller than the Reynolds stresses, although they can be comparable and even exceed the latter in very steep vortex waves generated by wind. Since this is related first and foremost to very short waves like ripples, which can influence the processes studied here only in a very thin surface layer, we shall not take this effect into account and approximately estimate the input of energy to turbulence from the waves as

$$P^w(z) \approx C_w u_*\frac{dE^w}{dz}. \tag{12}$$

We present the contribution of energy from a single breaking wave as

$$P^{br}(z) = \frac{d}{dz}\left(\nu^{br}\frac{dE^{br}}{dz}\right), \tag{13}$$

where ν^{br} and E^{br} are the turbulent viscosity coefficient and kinetic energy in the zone of breaking waves, respectively. Let us use the concepts about the wave breaking process as the motion of an aerated jet penetrating under the surface [21] to estimate these values. The authors of this publication consider the motion of two-phase fluid on the basis of the theory of turbulent jets and determine the velocity and energy variations of such a jet with depth. The turbulent viscosity coefficient in the breaking wave zone is estimated according to the Prandtl's formula:

$$\nu^{br} = \chi u_m^{br} b, \tag{14}$$

where u_m^{br} is the velocity at the axis of the jet, b is half-width of the jet, and $\chi \approx 0.1$ is a constant. Assuming the universality of velocity profiles in the jet, we can find

the mean energy in the horizontal section by integrating across the jet as follows:

$$E^{br} = \frac{1}{b}\int_0^b u^2 dy = a\left(u_m^{br}\right)^2, \quad (15)$$

where $a \approx 0.286$ [22]. Taking into account the fact that the jet widens linearly [22] and the velocity in an aerated jet decreases according to the following law [21]

$$u_m^{br} = u_0\left(1 + C_j\frac{z}{b_0}\right)^{-0.6}, \quad (16)$$

where u_0 is the velocity at the initial section of the jet and $2b_0$ is the width of the breaking wave crest, we finally get

$$P^{br} = C_{br}\frac{u_0^3}{b_0}\left(1 + C_j\frac{z}{b_0}\right)^{-2.8}. \quad (17)$$

The values of constants are $C_{br} \approx 1.5 \times 10^{-3}$; $C_j \approx 6.75$ [21, 22]. The values can become more exact as the model is verified. We consider that the jet is completely turbulized at the initial section already; therefore, the depth is calculated from the surface. The initial velocity in the jet according to [23] is determined from the phase velocity of the wave as $u_0 \approx 1.12c_p$, and the width of the breaking wave crest is estimated from the empirical dependence as a function of wind velocity at a height of 10 m [24]:

$$2b_0 = 8.5 \times 10^{-3} V_{10}. \quad (18)$$

The probability of wave breaking is related in [25] to the phase velocity of waves and friction velocity in air using an empirical dependence

$$q = -2.47 + 32.87\left(u_*^a\right)^2 + 42.37\frac{u_*^a}{c_p}. \quad (19)$$

Thus, we determined all input variables in Eqs. (8) and (9) other than the unknown variables E_{P2} and ε_{P2}. The system is closed in a usual manner, like in the first case.

The energy is not transferred directly from the first scale range to the third (transition range $k_2 \le k \le k_3$). The energy input occurs only from the second range. Here it is transferred through a cascade to the range of small scales (the dissipation range). The equation system for the third range is written as

$$\varepsilon_{P2} + \frac{d}{dz}\left(\frac{\nu_1^t}{\sigma_E}\frac{dE_{T3}}{dz}\right) - \varepsilon_{T3} = 0, \quad (20)$$

$$C_5\frac{\varepsilon_{P2}\varepsilon_{T3}}{E_{T3}} + \frac{d}{dz}\left(\frac{\nu_1^t}{\sigma_\varepsilon}\frac{d\varepsilon_{T3}}{dz}\right) - C_6\frac{\varepsilon_{T3}^2}{E_{T3}} = 0. \quad (21)$$

The notations here are the same as before. The closure is the same as in the previous cases. We accept the coefficient from the first range as the coefficient of turbulent exchange, because turbulent transfer would be generally determined by large vortices formed in the first scale range.

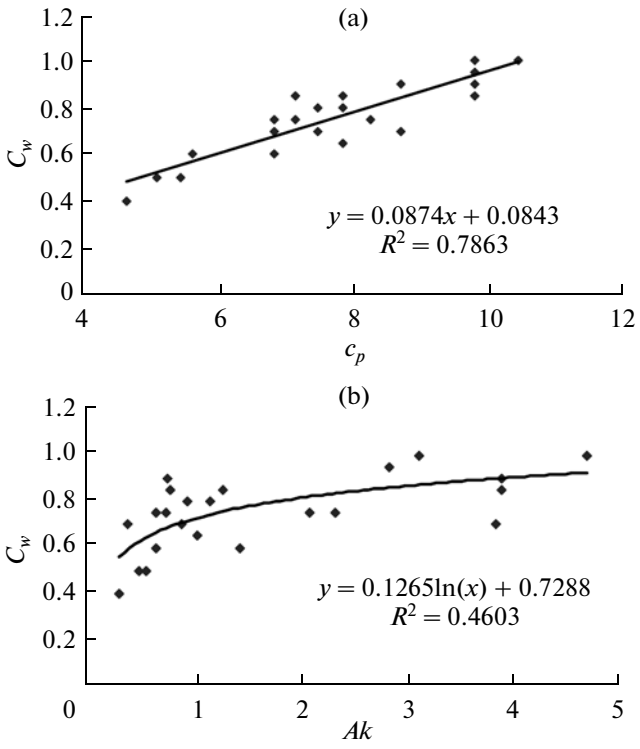

Fig. 2. Coefficient C_w characterizing the input of wave energy to turbulence versus wave parameters: (a) velocity of the spectral peak c_p and (b) wave steepness Ak (A is amplitude and k is wave number). Approximating equations and determination coefficients (squared cross correlation) R^2 are also shown on the graphs.

Finally, in the fourth range we simply have

$$\varepsilon_{T3} = \varepsilon, \quad (22)$$

i.e., the entire energy leaving the third range dissipates.

METHOD OF SOLUTION

All previously described equation systems were solved numerically using a finite-difference method with a standard scheme [26] and a uniform grid. After a transition to dimensionless values, Eqs. (4)–(5), (8)–(9), and (20)–(21) were substituted by the difference analogs over a three-node template. The corresponding nonlinear system was solved using the sweep method and iterations. At first, the values of ν were calculated at specified initial distributions of E and ε. Linearization of the system was performed by substituting the calculated coefficients ν^t. Convergence of the calculation was estimated by means of stabilizing the calculated values (when the value after a new iteration differed from the previous one by no more than 0.01%).

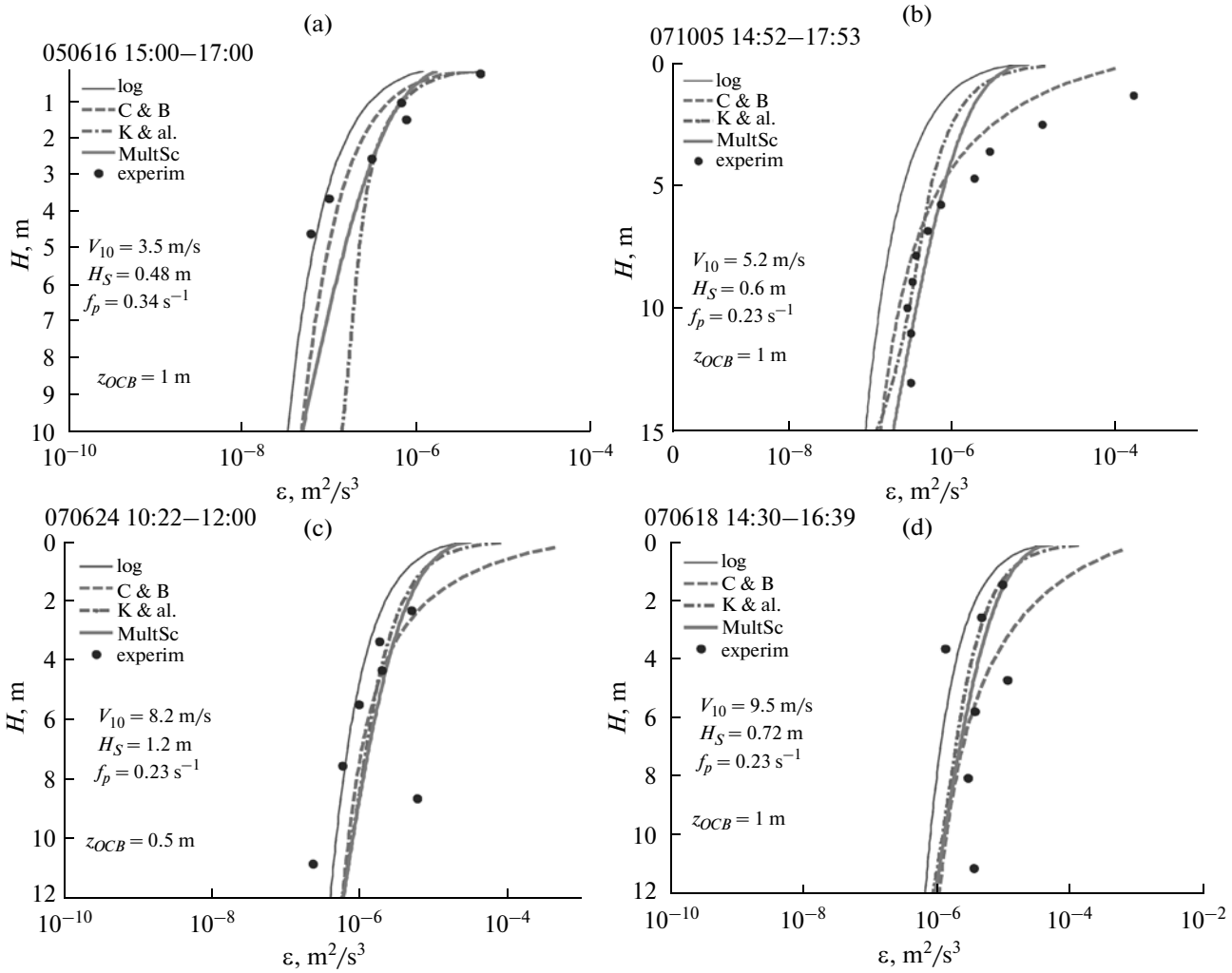

Fig. 3. Rate of turbulent-energy dissipation versus depth: comparison of model and experimental data at different hydrometeorological conditions. Along with the calculations using the multiscale model (MultSc), calculations using other models are also shown: for near-wall turbulence (log), the Craig and Banner model (C&B) [4, 5], and Kudryavtsev with coauthors model (K&al.) [14], the dots show experimental values; V_{10} is wind velocity at a height of 10 m, H_s is the height of significant waves, f_p is the wave frequency of the spectral peak, and z_{OCB} is the roughness parameter in the C&B model.

RESULTS OF MODELING AND VERIFICATION OF THE MODEL

The main problem in the division of the spectrum into ranges is to determine the boundary wave numbers k_1, k_2, k_3. It is reported in [15] that the exact location of the separation point does not significantly influence the results of calculation if the coefficients are selected correctly. One peculiarity of our approach is the fact that coefficients in Eq. (4)–(5), (8)–(9), and (20)–(21) are not completely independent. They are selected with the account for the ratio of energy values and transfer rates in different ranges: E_{P1}/E_{P2}, $\varepsilon_1/\varepsilon_2$, and similar ones. In other words, the boundary between the ranges is not rigid. Thus, the selection of coefficients would depend on the form of the power spectrum, which is determined by the ratios between energy levels or eventually by the conditions at the sea surface. The dependence of coefficients on these ratios allows us to take into account the influence of the vortices of medium and small scales on the larger ones, i.e., the feedback [15].

Since velocity shear was considered the only mechanism of turbulence generation in the first scale range, the coefficients in this range (rounded off to tenths) were taken according to the recommendation for such currents [18]. The results of calculations demonstrated that in our case the coefficients for the third range do not have a significant influence on the result. They were taken constant and most attention was focused on the influence of waves on turbulization and energy redistribution between the first, second, and third ranges. In this stage of model testing, we did not take into account the complex interactions between wind and waves. The resistance coefficient of the surface c_D was taken equal to 0.0015. The largest part of

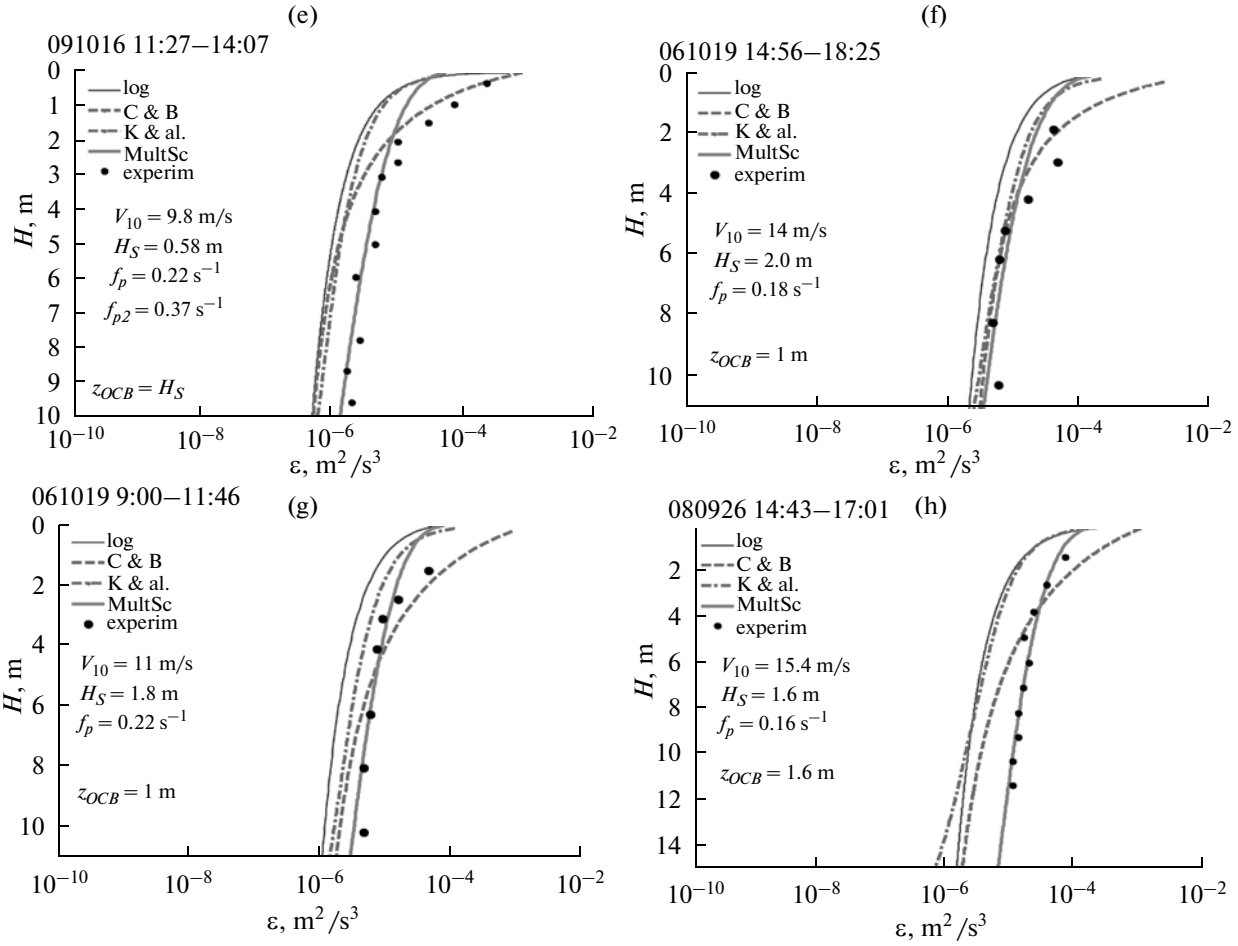

Fig. 3. Contd.

constants in equations (4)–(5), (8)–(9), and (20)–(21) were universal for all analyzed hydrometeorological situations. We varied only constants C_w and C_4.

Figure 2 shows the dependences of coefficient C_w on the wave parameters. The coefficient was selected so that the calculations would agree best of all with the experimental data. The coefficient characterizes the energy input from the waves due to the interaction with turbulence. We see that there is a correlation with the phase velocity of the spectral peak; the correlation with the steepness of the wave is less pronounced. Constant C_4 is inversely dependent on C_w; it varied within 0.4–1.2. We give a list of constants used in the calculations: $C_1 = 1.5$, $C_2 = 2.0$, $C_3 = C_5 = 0.01$, $C_6 = \sigma_E = 1.0$, $\sigma_\varepsilon = 1.3$ for the first range and $\sigma_\varepsilon = 1.0$ for the second and third ranges.

We used experimental data to compare with the calculations. They were obtained in field experiments on an oceanographic platform near Katsiveli [27, 28] in the coastal zone over a number of years. A brief description of the measuring equipment and methods for calculating the turbulent-energy dissipation rate are given in the Appendix.

Since not all processes influencing the turbulence are considered in the model suggested here, we selected comparatively common hydrometeorological situations close to classic ones for selecting the coefficients for estimates: neutral stratification, the same direction of the wind and waves, and lack of visible manifestation of the Langmuir circulations. In such situations, it was generally not difficult to select the applicable values for coefficients to gain an agreement between the calculations and experiments.

Figure 3 shows experimental values of the dissipation rate and model calculations. Calculations using other models are also shown for comparison. The main average hydrometeorological characteristics during the experiments are shown in the figures. The model of shear turbulence for the logarithmic layer denoted in the figures as "log" was calculated using formula (1). In the model of Craig and Banner (C&B), the roughness parameter z_0 was selected for each case with the coefficients that were recommended in their article; the model of Kudryavtsev et al., was calculated in its original form [14].

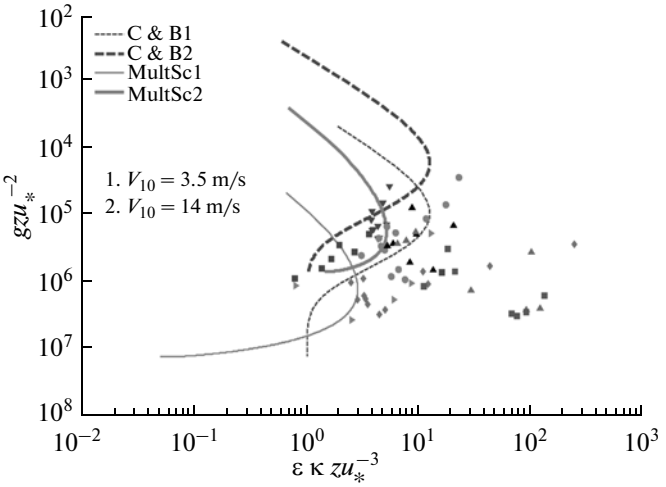

Fig. 4. Normalized dissipation rates versus dimensionless depth. Dashed lines denote the C&B model; solid lines denote the multiscale model. Thin lines correspond to $V_{10} = 3.5$ m/s; thick lines correspond $V_{10} = 14$ m/s.

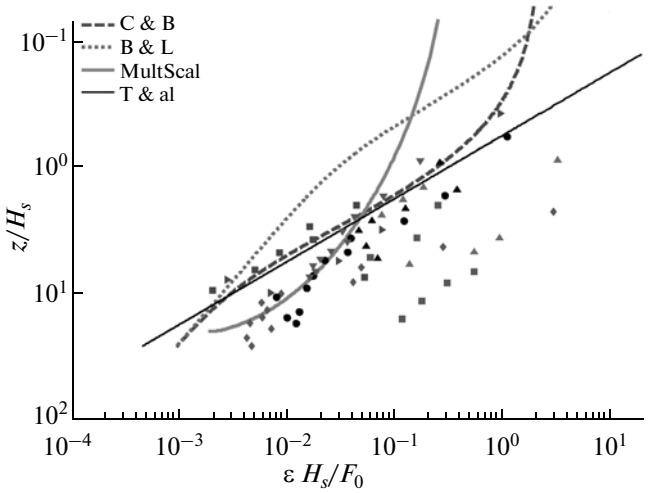

Fig. 5. Dissipation rates normalized by the energy flux to waves versus dimensionless depth. Dashed lines denote the C&B model, dotted lines denote the Benilov and Ly model (B&L), the thick solid line denotes the multiscale model, and the thin line is the empirical dependence [3].

It is seen from the figures that the multiscale model suggested here sufficiently satisfied the field data in the examples presented. The difference with other models is especially manifested in the storm conditions when dissipation strongly exceeds the theoretical values for the near-wall layer and decreases more slowly with depth (Figs. 3e–3h), whereas the multiscale model seems preferable. In a number of cases, a coincidence between the calculated and experimental values was not gained. However, in such cases we usually could indicate the possible cause of this discrepancy: the existence of increased local gradients of the current velocity, opposing directions of waves and swell, the appearance of Langmuir circulation, etc. The calculations with other models also did not agree with the experiment. The most discrepancies were observed at low winds when all models demonstrated sufficiently lower dissipation rates.

A satisfactory agreement between the theoretical curves and the values is observed in Fig. 3a, but the form of the experimental depth dependence of ε slightly differs from the model. It is possible that the degree of wave development can play a role in this case because at depths below 3 m turbulence is determined by the velocity shear ("log" curve), whereas above it the role of waves is present. It is likely that the same factor (degree of wave development) and local gradients of the current velocity are the reasons for scattering of the experimental dots also in the cases shown in Figs. 3c and 3d. The C&B model in Fig. 3b gives the best coincidence, which was gained by selecting z_0. There was a peculiar hydrometeorological situation: the wind direction was opposite the propagation of light swell. It is likely that this made an additional contribution to turbulence from the tangential wind stress. It can be seen in Figs. 3e, 3f, and 3g that the agreement between the multiscale model and the experiment in the upper 2- to 3-m-thick layer is not very good. We already noted that a possible reason for this effect is the more complicated mechanisms of interaction between waves, current, and turbulence and the variability of the coefficient of the surface resistivity c_D, which was considered constant in the model. These effects manifest themselves to a greater extent near the surface. In addition, the situation shown in Fig. 3e is characterized by the existence of two systems of surface waves (the second peak on the spectrum at $f_{p2} = 0.37$ Hz), which likely causes increased turbulization in the layer above 2 m.

Figures 4 and 5 show experimental and model values of ε in dimensionless coordinates (that correspond to the data in Figs. 3a–3h) normalized by different methods: by the energy flux directly going to the ocean and the energy flux to the waves, which are usually used in such cases [14]. It is seen from the figures that these normalizations cannot be considered universal for all cases.

This model allows us to calculate the variations of the turbulent energy over individual spectral ranges. Figure 6 shows examples of such calculations for different conditions. The relative amount of turbulent energy that circulates in the spectral ranges considered here changes depending on the hydrometeorological situation. This explains the scattering of dots in Figs. 4 and 5: in different situations and at different depths, dissipation can be determined by the energy input from different sources of turbulence.

CONCLUSIONS

We can conclude on the basis of model calculations and their comparison with the experimental data that

Technical characteristics of the Sigma-1 measuring complex

Measured parameters	Range	Resolution	Accuracy	Frequency of measurements
Three components of velocity pulsations	±2 m/s	10^{-3} m/s	±10%	100 Hz for all channels
Temperature	0–30°C	0.001°C	±5%	
Relative electric conductivity	0–0.9	2.5×10^{-5}	±5%	
Three components of linear accelerations	±2g	0.002 m/s^2	0.002 m/s^2	
Roll and pitch	±20°	0.01°	±1°	
Azimuth	0°–360°	1.0°	±5°	
Pressure	0–1 MPa	5×10^{-4}	±1%	

this approach to turbulence modeling in the upper layer generally results in good correspondence between the calculations and experiments. It is especially pronounced at strong winds and developed waves, whereas the other models in these situations result in discrepancies with the experiment as the distance from the surface increases. This model has a number of advantages when compared with the other models: the turbulence structure is described more adequately, turbulence generation by different mechanisms is taken into account at the corresponding scales, and nonequilibrium generation and dissipation in different spectral ranges are taken into account.

Other than the mentioned positive features, the model has a number of simplifications, which could have influenced the result to some extent. In this form, the model is not completely adjusted to all complex and diverse processes which occur near the sea surface. For example, the model did not take into account the variability of the coefficient of surface resistance c_D, which strongly influences the results of calculation. The model does not take into account the influence of waves on the velocity shear, vortex structures in the waves, coherent structures, etc. The realistic wave spectrum and fluxes of heat and buoyancy were not included in the model. Nevertheless, in the cases when these mechanisms do not have a significant influence on the turbulent regime, the model adequately describes the distribution of dissipation and allows us to parameterize the vertical turbulent exchange sufficiently well.

At present we can determine how we can improve the model: account for other turbulence sources and the introduction of new terms in the equations in the corresponding ranges, as well as the selection of "correct" coefficients in each range with account for a deep understanding of the physics of different processes at the given scales. There is another possibility of improving the model: the application if necessary a larger number of ranges in the division of the spectrum.

APPENDIX

Sigma-1 Measuring Complex for Investigating Turbulence near the Sea Surface and the Method to Determine the Dissipation Rate of Turbulent Energy.

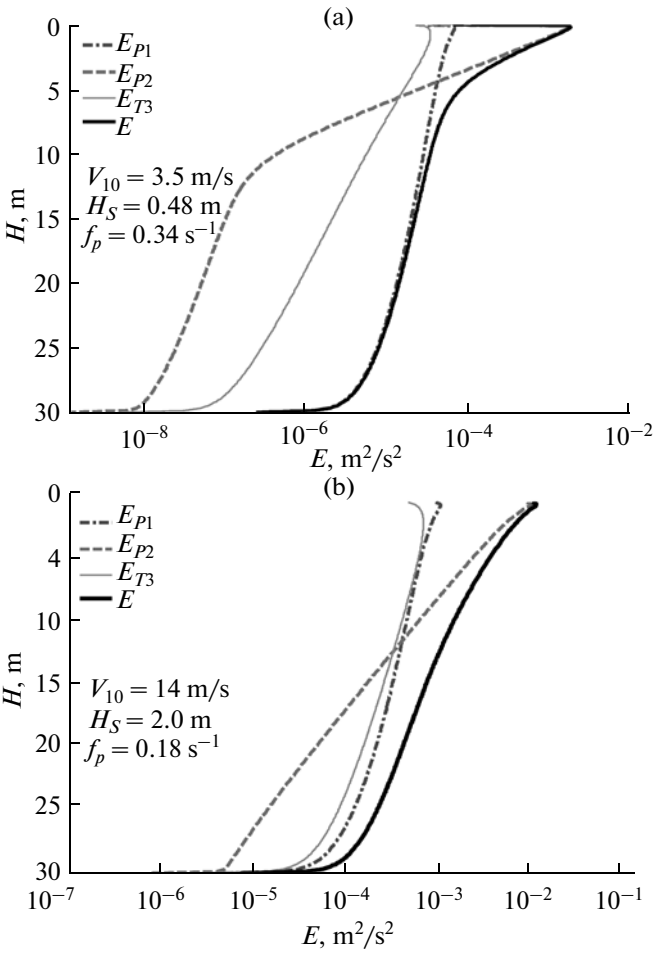

Fig. 6. Levels of turbulent energy based on the multiscale model in different spectral ranges at different hydrometeorological conditions. The thick solid line denotes the total turbulent energy (E).

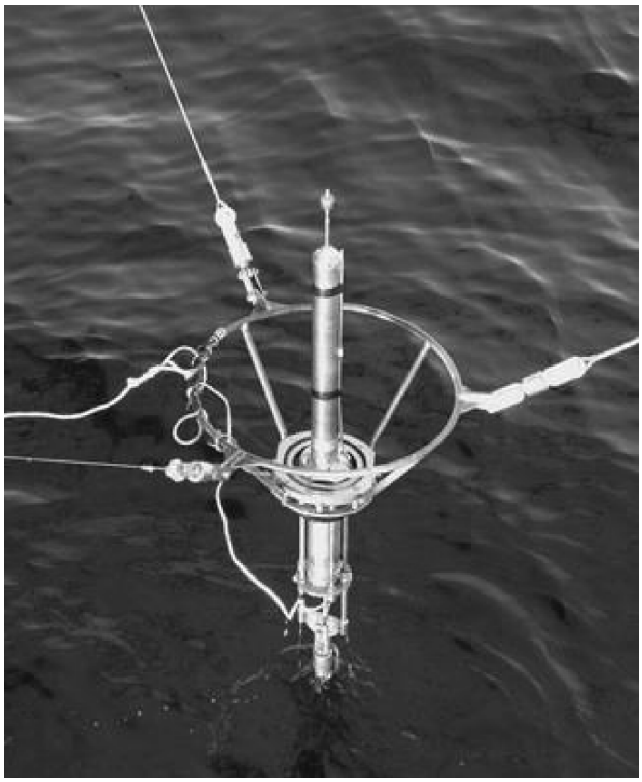

Fig. 7. Measuring complex Sigma-1. A point-to-point version.

We are used a point-to-point version of the Sigma-1 measuring complex [29] in the experimental investigations of the turbulent regime in the surface layer. A general view of the complex is shown in Fig. 7, and its technical characteristics are given in Table 1. The measuring complex is connected by a cable to the deck unit. Information is recorded and accumulated by a personal computer on a real-time basis. A system was developed for positioning the complex that makes minimizing possible oscillations of the instrument possible and at the same time offers an operative change of the measurement horizon in the range from 0 to 20 m. The measuring device is located at a distance from the platform, which eliminates the influence of the pillars on the region of measurements and ensures that data are measured in a natural medium. The measurements are carried out on the open sea side during the corresponding direction of currents to avoid the influence of the platform. The rate of dissipation of turbulent energy ε was calculated using the method suggested in [30]; it was also described in [9]. The distortions of the signal due to waves and oscillations of the instrument on the suspension do not strongly influence the result. The dissipation rate was determined similarly in [31]. The method is based on the hypothesis of Kolmogorov, according to which the spectral density of velocity pulsations can be presented as

$$E(k) = \varepsilon^{1/4}\nu^{5/4}F(\lambda), \qquad (23)$$

where k is the wave number, ν is kinematic viscosity, $F(\lambda)$ is a universal function (model spectrum), and $\lambda = k/(\varepsilon^{1/4}\nu^{-3/4})$ is the dimensionless wave number. A straight line with a slope of +1 is plotted on the experimental spectrum in the logarithmic scale: $\log E(k) = \log \nu^2 k$. The theoretical spectrum is also plotted in the logarithmic scale and point (0,0) is marked on the graph. Then the graphs are aligned for the better coincidence between the experimental and model curves. The dissipation rate was estimated from the coordinates of the marked point, which should be located on the straight line. Kinematic viscosity was calculated from the measured temperature and salinity; the Nasmith spectrum was used as a model [32]. The measured pulsation values were first processed by a median filter, then the frequency spectrum was calculated and recalculated to the wave number spectrum based on the Taylor's hypothesis of frozen turbulence: $U_d = \omega/k$, where k is the wave number, U_d is the transport velocity of turbulent eddies through the sensor, and ω is the angular frequency. The mean velocity of the main current was assumed as the transport velocity. We used the values of ε to compare with the model. The values were calculated from the pulsations of vertical velocity as less subjected to the influence of the natural oscillations of the instrument.

REFERENCES

1. Y. C. Agrawal, E. A. Terray, M. A. Donelan, P. A. Hwang, A. J. Williams III, W. M. Drennan, K. K. Kahma, S. A. Kitaigorodskii, "Enhanced dissipation of kinetic energy beneath breaking waves," Nature **359** 219–220 (1992).
2. S. A. Kitaigorodskii, M. A. Donelan, J. L. Lumley, and E. A. Terray, "Wave-turbulence interaction in the upper ocean. Part II: Statistical characteristics of wave and turbulent components of the random velocity field in the marine surface layer," J. Phys. Oceanogr. **13**, 1988–1999 (1983).
3. E. A. Terray, M. A. Donelan, Y. C. Agrawal, W. M. Drennan, K. K. Kahma, A. J. Williams III, P. A. Hwang, S. A. Kitaigorodskii, "Estimates of kinetic energy dissipation under breaking waves," J. Phys. Oceanogr. **26** (5), 792–807 (1996).
4. P. D. Craig and M. L. Banner, "Modelling wave-enhanced turbulence in the ocean surface layer," J. Phys. Oceanogr. **24** (12), 2546–2559 (1994).
5. P. P. Craig and M. L. Banner, "Velocity profiles and surface roughness under breaking waves," J. Geophys. Res. **101** (C1), 1265–1277 (1996).
6. S. A. Kitaigorodskii, "On the influence of wind wave breaking on the structure of the subsurface oceanic turbulence," Izv., Atmos. Ocean. Phys. **37** (4), 525–535 (2001).
7. A. Anis and J. N. Moum, "Surface wave-turbulence interactions: scaling $\varepsilon(z)$ near the sea surface," J. Phys. Oceanogr. **25** (9), 2025–2045 (1995).

8. F. Ardhuin and A. D. Jenkins, "On the interaction of surface waves and upper ocean turbulence," J. Phys. Oceanogr. **36** (3), 551–557 (2006).
9. A. S. Monin and R. V. Ozmidov, *Oceanic Turbulence* (Gidrometeoizdat, Leningrad, 1981) [in Russian].
10. T. Kukulka, T. Hara, and S. E. Belcher, "A model of the air–sea momentum flux and breaking-wave distribution for strongly forced wind waves," J. Phys. Oceanogr. **37** (7), 1811–1828 (2007).
11. R. J. Gemmrich and D. M. Farmer, "Near-surface turbulence and thermal structure in a wind-driven sea," J. Phys. Oceanogr. **29** (3), 480–499 (1999).
12. A. Y. Benilov and L. N. Ly, "Modeling of surface waves breaking effects in the ocean upper layer," Math. Comput. Modell. **35** (1), 191–213 (2002).
13. A. M. Chukharev, "Contributions of unbreaking wind waves and the velocity shear of a drift flow to turbulent exchange," Izv., Atmos. Ocean. Phys. **39** (5), 607–613 (2003).
14. V. Kudryavtsev, V. Shrira, V. Dulov, and V. Malinovsky, "On the vertical structure of wind-driven sea currents," J. Phys. Oceanogr. **38** (10), 2121–2144 (2008).
15. K. Hanjalić, B. E. Launder, and R. Schistel, "Multiple-time-scale concepts in turbulent transport modeling," in *Turbulent Shear Flows 2, Selected Papers from the Second International Symposium on Turbulent Shear Flows,* Ed. by L. J. S. Bradbury, F. Durst, B. E. Launder, F. W. Schmidt, and J. H. Whitelaw (Springer, Berlin–Heidelberg–New York, 1980), pp. 36–49.
16. R. V. Ozmidov, "Some specific features of the energetic spectrum of oceanic turbulence," Dokl. Akad. Nauk USSR **161** (4), 828–831 (1965).
17. S. A. Kitaigorodskii and J. L. Lumley, "Wave-turbulence interaction in the upper ocean. Part I," J. Phys. Oceanogr. **13**, 1977–1987 (1983).
18. W. Rodi, "Turbulence models for environmental problems," in *Prediction Methods for Turbulent Flows*, Ed. by W. Kollmann (Hemisphere Publishing Corporation, Washington, 1980), pp. 259–349.
19. V. N. Kudryavtsev and V. Makin, "Impact of swell on marine atmospheric boundary layer," J. Phys. Oceanogr. **34**, 934–946 (2004).
20. T. K. Cheung and R. L. Street, "The turbulent layer in water at an air–water interface," J. Fluid Mech. **194** (9), 133–151 (1988).
21. A. M. Chukharev and B. B. Kotovshchikov, "Effect of breaking surface waves on turbulent exchange. Spilling breakers," Morsk. Gidrofiz. Zh., No. 3, 13–19 (2000).
22. A. S. Ginevskii, *Teory of Turbulent Jets and Wakes* (Mashinostroenie, Moscow, 1969) [in Russian].
23. M. S. Longuet-Higgins and J. S. Turner, "An "entraining plume" model of a spilling breaker," J. Fluid Mech. **63** (1),1–20 (1974).
24. W. K. Melville and P. Matusov, "Distribution of breaking waves at the ocean surface, Nature **417** (5), 58–63 (2002).
25. K. B. Katsaros and S. S. Atakturk, "Dependence of wave breaking statistics on wind stress and wave development," in *Breaking Waves*, Ed. by M. L. Banner and R. H. J. Grimshaw, (Springer, 1992), pp. 119–132.
26. A. A. Samarskii, *Difference Schema Theory* (Nauka, Moscow, 1977) [In Russian].
27. A. M. Chukharev, V. A. Barabash, A. G. Zubov, and O. I. Pavlenko, "Turbulent structure of near-surface sea layer according to data of Sigma-1 measuring system," Morsk. Gidrofiz. Zh., No. 2, 15–28 (2007).
28. A. M. Chukharev, "Field measurements of dissipation of turbulent kinetic energy in the near-surface sea layer," in *Ecological Safety and Integrated Use of Coastal and Shelf Zones of the Sea* (Marine Hydrophysical Institute of the National Academy of Ukraine, Sevastopol, 2010), No. 21, pp. 124–135 [in Russian].
29. A. S. Samodurov, V. Z. Dykman, V. A. Barabash, O. I. Efremov, A. G. Zubov, O. I. Pavlenko, A. M. Chukharev, "Sigma-1 measuring system for studying the small-scale characteristics of hydrophysical fields in the upper sea layer," Morsk. Gidrofiz. Zh., No. 5, 60–71 (2005).
30. R. W. Stewart and H. L. Grant, "Determination of the rate of dissipation of turbulent energy near the sea surface in the presence of waves," J. Geophys. Res. **67** (8), 3177–3180 (1962).
31. A. Soloviev and R. Lucas, "Observation of wave-enhanced turbulence in the near-surface layer of the ocean during TOGA COARE," Deep-Sea Res. **50** (2), 371–395 (2003).
32. N. H. Oakey, "Determination of the rate of dissipation of turbulent energy from simultaneous temperature and velocity shear microstructure measurements," J. Phys. Oceanogr. **12** (3), 256–271 (1982).

Translated by E. Morozov